Time domain analysis for PWM mode of CLLLC converter

Dohong Lee
Dept of Electrical and Electronics Engineering
Konkuk University
Seoul, Republic of korea
Leedohong@konkuk.ac.kr

Bonggook Kim
Dept of Electrical and Electronics Engineering
Konkuk University
Seoul, Republic of korea
Fbk0401@konkuk.ac.kr

Xuanxi Liu
Dept of Electrical and Electronics Engineering
Konkuk University
Seoul, Republic of korea
Xixi311@konkuk.ac.kr

Younghoon Cho
Dept of Electrical and Electronics Engineering
Konkuk University
Seoul, Republic of korea
Yhcho98@konkuk.ac.kr

2024 IEEE Energy Conversion Congress and Exposition (ECCE) | 979-8-3503-7606-7/24/$31.00 ©2024 IEEE | DOI: 10.1109/ECCE55643.2024.10861224

***Abstract*—This paper presents a comprehensive time domain analysis for the Pulse Width Modulation (PWM) mode of CLLLC converters. The analysis involves deriving state equations for different operational modes and solving them to obtain voltage and current waveforms. The model's validity is confirmed through both simulation and experimental results, which show a high degree of correlation. Despite minor asymmetries and operational point variations in the actual resonant network, the model proves robust and applicable. This work provides a suitable tool for the design and analysis of PWM CLLLC converters, enhancing their efficiency and performance in practical applications.**

Keywords—CLLLC, PWM, Resonant converter, DC-DC

I. INTRODUCTION

ISOLATED dc-dc converter is the main stream in applications, such as electric vehicle, micro grid, energy storage systems, solid state transformer, and so on. Among isolated dc-dc converters, CLLC class topology are widely used to the applications due to their powerful advantages such as bidirectional operation capability, high efficiency, high power density, soft switching characteristic, wide gain range [1], [2].

For EV charger system, major design consideration is the wide output gain range. In general, the resonant converters are designed by adjusting the resonant frequency of the resonant network, quality factor, and turn ratio of the transformer, considering the output range of the converter. To achieve a wide output gain range of CLLC converters by variable frequency operation, the magnetizing inductance of the transformer needs to be designed with a small value [3]. As a result, the further the operating point of the CLLC converter moves from the resonant point, the more the circulating current increases, leading to a significant decrease in efficiency. To compensate for these shortcomings, Several studies have been conducted using Phase-Shift Modulation (PSM) [4], [5]. However, even when applying PSM along with variable frequency operation, there are limitations in operating the converter over a wide output range of several hundred volts. Recently, To widen additional voltage gain range, the resonant converter with Pulse-width-modulation has been studied[6], [7]. These PWM provides the converter with additional switching states, which can extend the output range of the converter [7]. For resonant converters utilizing PWM techniques, traditional methods like first harmonic approximation and extended harmonic approximation are not suitable. It is because the resonant currents and voltages are neither sinusoidal nor symmetrical. In addition, According to the PWM method, the switching state is asymmetric, which makes it difficult to interpret the converter operation.

This paper proposes the time domain analysis for PWM mode of CLLLC converter. In section II, PWM mode operation of CLLLC converter is described. In section III, Time domain modeling for PWM mode CLLLC converter is conducted.

II. PWM MODE OPERATION OF THE CLLLC CONVERTER

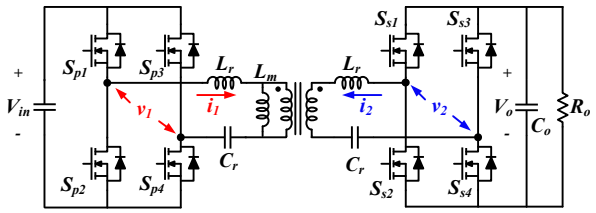

Fig. 1. Circuit diagram of the CLLLC converter

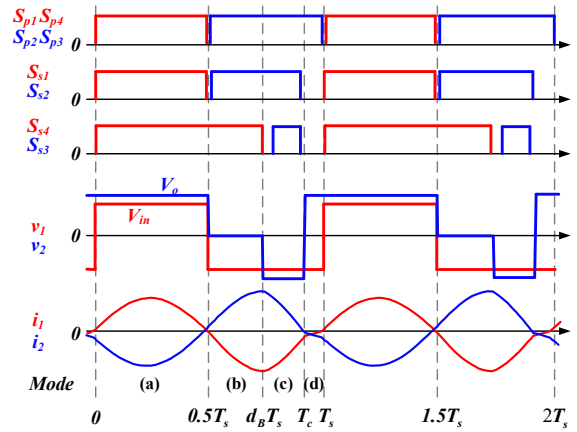

Fig. 2. Theoretical waveforms of PWM mode CLLLC converter.

Figure 1 and 2 represent the summary of PWM operation of CLLLC converter. The L_r, C_r, and L_m represent the resonant inductor, the resonant capacitor, and the magnetizing inductance of the transformer. Also, Co and Ro represent the output capacitor and the load resistance. Besides, T_s and d_B represents the switching cycle of the CLLLC converters and the duty ratio of switch S_{s4}, respectively.

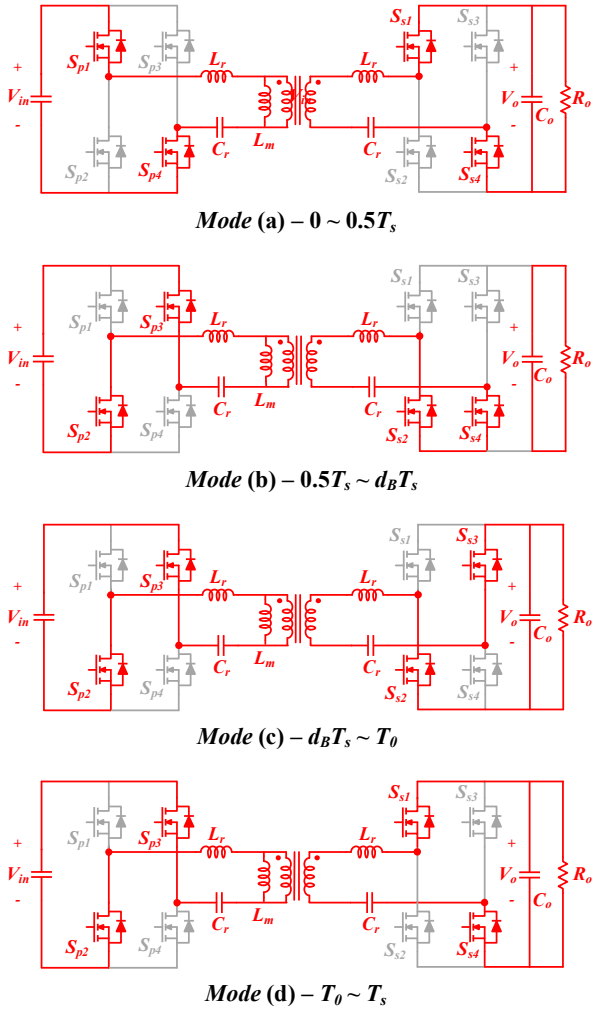

Fig. 3. The conduction path of PWM Operation in CLLLC Converters.

Compared with the variable frequency resonant CLLLC converter, the secondary side converter of PWM mode CLLLC is modulated to boost the output voltage. During for half a cycle in *Mode* (a), the converter operates as a typical resonant converter. Thereafter, the PWM mode CLLLC converter enters *Mode* (b) where the resonant current of the converter rises in the negative direction. In this mode, the energy supplied from the input side accumulates in the resonant network. The longer the duration of *Mode* (b), the higher the output voltage that can be achieved. Subsequently, the operation of the converter leads to the rectification *Mode* (c) until the secondary side resonant current i_2 becomes near zero. Lastly, the remainder switching period that small current freewheels through the switches S_{p2}, S_{p3}, S_{s1}, S_{s4} follows. The output voltage can be adjusted by d_B, and T_0 is determined by the operation point of the converter according to the operating voltage and power.

III. Time Domain Analysis for PWM Mode CLLLC Converter

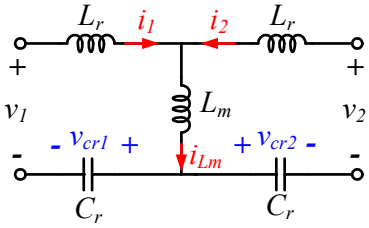

Fig. 4. Simplified resonant network for CLLLC converter.

Figure 4 shows simplified resonant network of the CLLLC converter. v_1 and v_2 are the primary and secondary side voltage of the resonant network. i_1 and i_2 means the primary and secondary resonant current. i_{Lm} represents the magnetizing current of the transformer. In the same way, v_{cr1} and v_{cr2} are the voltage of the primary and secondary side resonant capacitor. The state equations for the resonant network can be expressed by

$$\begin{cases} v_1 = L_r \dfrac{di_1}{dt} + L_m \dfrac{d(i_1+i_2)}{dt} + v_{cr1} \\ v_2 = L_r \dfrac{di_2}{dt} + L_m \dfrac{d(i_1+i_2)}{dt} + v_{cr2} \end{cases} \quad \begin{cases} i_1 = C_r \dfrac{dv_{cr1}}{dt} \\ i_2 = C_r \dfrac{dv_{cr2}}{dt} \end{cases} \tag{1}$$

If the input and output capacitance are large enough, the voltage v_1 and v_2 can be regarded as constant value in each *Mode* (a)~(d) in Figure 3. As taking sum and difference, equation (1) can be derived to (3) by (2).

$$\begin{cases} v_{crd} = v_{cr1} - v_{cr2} \\ v_{crs} = v_{cr1} + v_{cr2} \\ i_d = i_1 - i_2 \\ i_s = i_1 + i_2 \end{cases} \quad \begin{cases} v_k = v_1 - v_2 \\ v_h = v_1 + v_2 \\ L_{rm} = L_r + 2L_m \end{cases} \tag{2}$$

$$\begin{cases} v_k = L_r \dfrac{di_d}{dt} + v_{crd} \\ i_d = C_r \dfrac{dv_{crd}}{dt} \end{cases} \quad \begin{cases} v_h = L_{rm} \dfrac{di_s}{dt} + v_{crs} \\ i_s = C_r \dfrac{dv_{crs}}{dt} \end{cases} \tag{3}$$

Equation (3) is well-known two-pair, second-order differential equations. From determining the voltage v_k and v_h on each mode, (3) can be solved. Table 1 shows the voltages

TABLE I. INPUT VOLTAGE OF THE STATE EQUATIONS ACCORDING TO PWM MODE

Mode [Period]	*Resonant network input voltage*			
	v_1	v_2	v_k	v_h
(a) [$0 \sim 0.5T_s$]	V_{in}	V_o	$V_{in} - V_o$ ($=V_{ka}$)	$V_{in} + V_o$ ($=V_{ha}$)
(b) [$0.5T_s \sim d_BT_s$)	$-V_{in}$	0	$-V_{in}$ ($=V_{kb}$)	$-V_{in}$ ($=V_{hb}$)
(c) [$d_BT_s \sim T_0$]	$-V_{in}$	$-V_o$	$-V_{in} + V_o$ ($=V_{kc}$)	$-V_{in} - V_o$ ($=V_{hc}$)
(d) [$T_c \sim T_s$]	$-V_{in}$	V_o	$-V_{in} - V_o$ ($=V_{kd}$)	$-V_{in} + V_o$ ($=V_{hd}$)

of each mode for PWM mode CLLLC converter. Using the voltage $v_{ka\sim d}$, $v_{ha\sim d}$ according to each mode, the time-domain solutions of (3) is summarized as follows:

TABLE II. INPUT VOLTAGE OF THE STATE EQUATIONS ACCORDING TO PWM MODE

Mode (a)	$\begin{cases} v_{crd}(t) = (V_{crd}(0) - v_{ka}) \cdot \cos \omega_r t + \omega_r L_r i_d(0) \cdot \sin \omega_r t + v_{ka} \\ i_d(t) = -C_r \omega_r (V_{crd}(0) - v_{ka}) \cdot \sin \omega_r t + i_d(0) \cdot \cos \omega_r t \\ v_{crs}(t) = (V_{crs}(0) - v_{ha}) \cdot \cos \omega_m t + \omega_m L_{rm} i_s(0) \cdot \sin \omega_m t + v_{ha} \\ i_s(t) = -C_r \omega_m (V_{crs}(0) - v_{ha}) \cdot \sin \omega_m t + i_s(0) \cdot \cos \omega_m t \end{cases}$
Mode (b)	$\begin{cases} v_{crd}(t) = (V_{crd}(\frac{T_s}{2}) - v_{kb}) \cdot \cos \omega_r \left(t - \frac{T_s}{2}\right) + \omega_r L_r i_d(\frac{T_s}{2}) \cdot \sin \omega_r \left(t - \frac{T_s}{2}\right) + v_{kb} \\ i_d(t) = -C_r \omega_r (V_{crd}(\frac{T_s}{2}) - v_{kb}) \cdot \sin \omega_r \left(t - \frac{T_s}{2}\right) + i_d(\frac{T_s}{2}) \cdot \cos \omega_r \left(t - \frac{T_s}{2}\right) \\ v_{crs}(t) = (V_{crs}(\frac{T_s}{2}) - v_{hb}) \cdot \cos \omega_m \left(t - \frac{T_s}{2}\right) + \omega_m L_{rm} i_s(\frac{T_s}{2}) \cdot \sin \omega_m \left(t - \frac{T_s}{2}\right) + v_{hb} \\ i_s(t) = -C_r \omega_m (V_{crs}(\frac{T_s}{2}) - v_{hb}) \cdot \sin \omega_m \left(t - \frac{T_s}{2}\right) + i_s(\frac{T_s}{2}) \cdot \cos \omega_m \left(t - \frac{T_s}{2}\right) \end{cases}$
Mode (c)	$\begin{cases} v_{crd}(t) = (V_{crd}(d_B T_s) - v_{kc}) \cdot \cos \omega_r (t - d_B T_s) + \omega_r L_r i_d(d_B T_s) \cdot \sin \omega_r (t - d_B T_s) + v_{kc} \\ i_d(t) = -C_r \omega_r (V_{crd}(d_B T_s) - v_{kc}) \cdot \sin \omega_r (t - d_B T_s) + i_d(d_B T_s) \cdot \cos \omega_r (t - d_B T_s) \\ v_{crs}(t) = (V_{crs}(d_B T_s) - v_{hc}) \cdot \cos \omega_m (t - d_B T_s) + \omega_m L_{rm} i_s(d_B T_s) \cdot \sin \omega_m (t - d_B T_s) + v_{hc} \\ i_s(t) = -C_r \omega_m (V_{crs}(d_B T_s) - v_{hc}) \cdot \sin \omega_m (t - d_B T_s) + i_s(d_B T_s) \cdot \cos \omega_m (t - d_B T_s) \end{cases}$
Mode (d)	$\begin{cases} v_{crd}(t) = (V_{crd}(T_0) - v_{kd}) \cdot \cos \omega_r (t - T_0) + \omega_r L_r \cdot i_d(T_0) \cdot \sin \omega_r (t - T_0) + v_{kd} \\ i_d(t) = -C_r \omega_r (V_{crd}(T_0) - v_{kd}) \cdot \sin \omega_r (t - T_0) + i_d(T_0) \cdot \cos \omega_r (t - T_0) \\ v_{crs}(t) = (V_{crs}(T_0) - v_{hd}) \cdot \cos \omega_m (t - T_0) + \omega_m L_{rm} i_s(T_0) \cdot \sin \omega_m (t - T_0) + v_{hd} \\ i_s(t) = -C_r \omega_m (V_{crs}(T_0) - v_{hd}) \cdot \sin \omega_m (t - T_0) + i_s(T_0) \cdot \cos \omega_m (t - T_0) \end{cases}$

$$where,\ \omega_r = \frac{1}{\sqrt{L_r C_r}},\ \omega_m = \frac{1}{\sqrt{L_{rm} C_r}}$$

Table II represents the time domain model for PWM mode CLLLC converter. Considering the physical operation of the resonant network, the voltage v_{crd}, v_{crs} and current i_d, i_s are continuous at the boundaries of each mode. From the continuous conditions, the end values of each mode represents the initial value of next mode.

$$\begin{cases} v_{crd}(\frac{T_s}{2}) = (V_{crd}(0) - v_{ka}) \cdot \cos \omega_r \frac{T_s}{2} + \omega_r L_r i_d(0) \cdot \sin \omega_r \frac{T_s}{2} + v_{ka} \\ i_d(\frac{T_s}{2}) = -C_r \omega_r (V_{crd}(0) - v_{ka}) \cdot \sin \omega_r \frac{T_s}{2} + i_d(0) \cdot \cos \omega_r \frac{T_s}{2} \end{cases} \tag{4}$$

$$\begin{cases} v_{crs}(\frac{T_s}{2}) = (V_{crs}(0) - v_{ha}) \cdot \cos \omega_m \frac{T_s}{2} + \omega_m L_{rm} i_s(0) \cdot \sin \omega_m \frac{T_s}{2} + v_{ha} \\ i_s(\frac{T_s}{2}) = -C_r \omega_m (V_{crs}(0) - v_{ha}) \cdot \sin \omega_m \frac{T_s}{2} + i_s(0) \cdot \cos \omega_m \frac{T_s}{2} \end{cases} \tag{5}$$

Equation (4) and (5) represent the relationship between the initial values at time zero and time $0.5T_s$. In the same way, an additional six relational expressions between initial values can be obtained. All relational expressions are summarized in the appendix. By combining the relational expressions, an initial value regarding the system operation point can be obtained.

$$\begin{cases} v_{cr1}(t) = \frac{1}{2}(v_{cs}(t) + v_{crd}(t)) \\ v_{cr2}(t) = \frac{1}{2}(v_{cs}(t) - v_{crd}(t)) \\ i_1(t) = \frac{1}{2}(i_s(t) + i_d(t)) \\ i_2(t) = \frac{1}{2}(i_s(t) - i_d(t)) \end{cases} \tag{6}$$

It can be shown that by finding the specific solutions of [v_{cs}, v_{cd}, i_s, i_d] in each mode, time domain model for all components can be taken.

IV. Simulation and Experimental Verification

A. Simulation verification

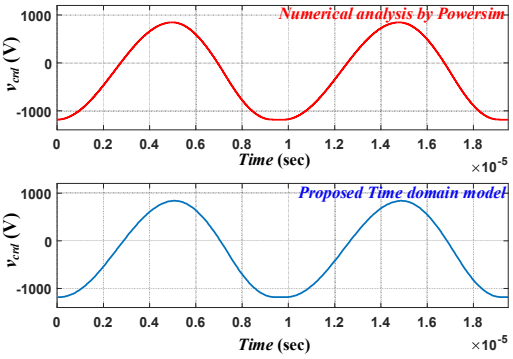

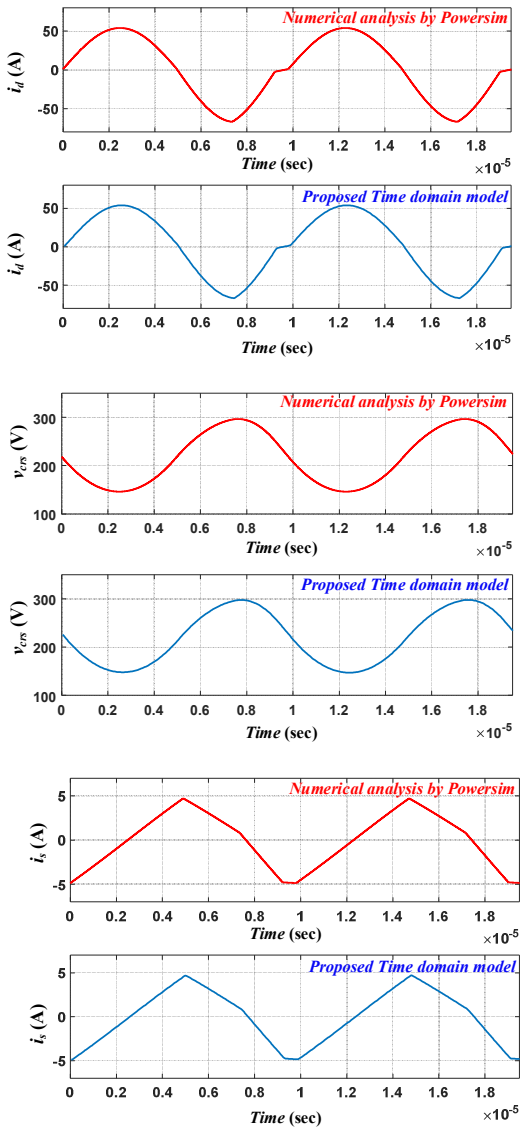

Fig. 5. Comparison of [v_{crd}, i_d, v_{crs}, i_s] between the proposed time domain model by MATLAB and simulation results by Powersim

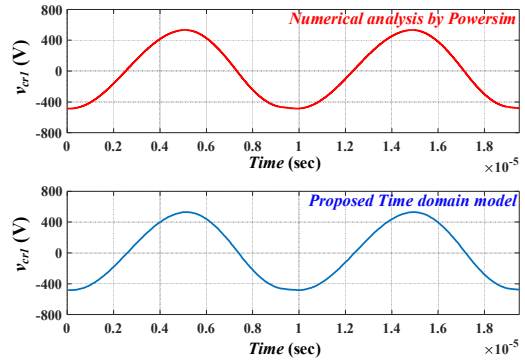

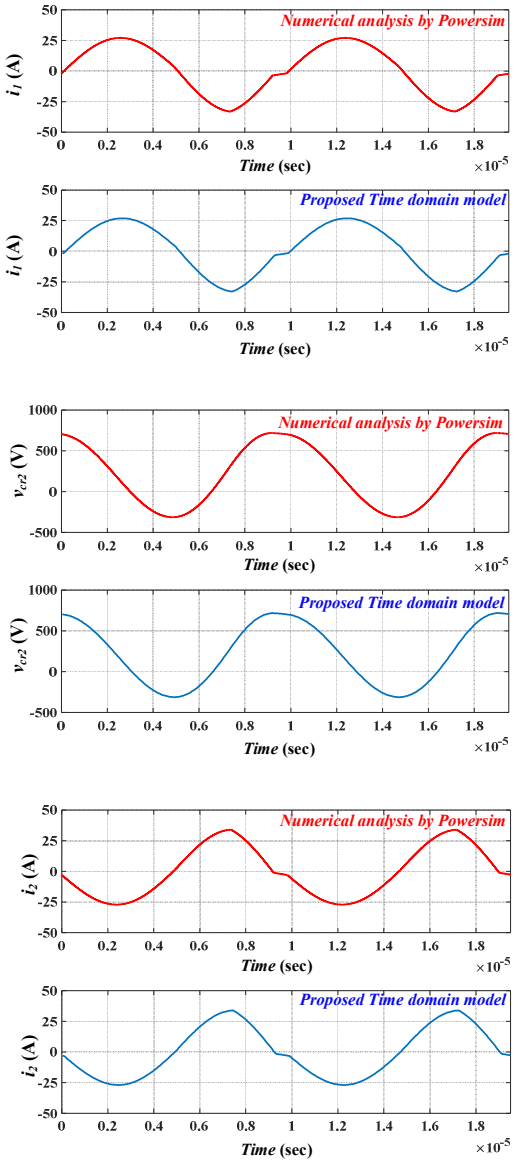

Fig. 6. Comparison of [v_1, i_1, v_2, i_2] between the proposed time domain model by MATLAB and simulation results by Powersim

Figure 5 and 6 show the comparison between the proposed time domain model by MATLAB and Powersim. The operating condition of comparison is summarized as Table III:

TABLE III
CIRCUIT PARAMETER FOR CLLLC CONVERTER MODEL

PARAMETER	Value
Rated operating power (P)	7.2 kW
Input voltage (V_{in})	420 V
Primary/secondary resonant inductor (L_r)	30 μH
Primary/secondary resonant capacitor (C_r)	85 nF
Magnetizing inductance (L_m)	190 μH
Switching frequency (f_s)	100 kHz
Turn ration of transformer (n)	1
Boost Duty ratio (d_B)	0.75

B. Experimental verification

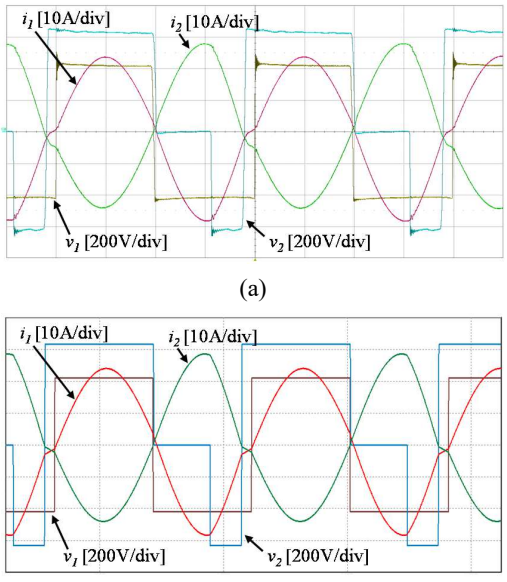

Fig. 7. Comparison of [v_1, i_1, v_2, i_2] between the experimental results and simulation (a) experimental results (b) simulation

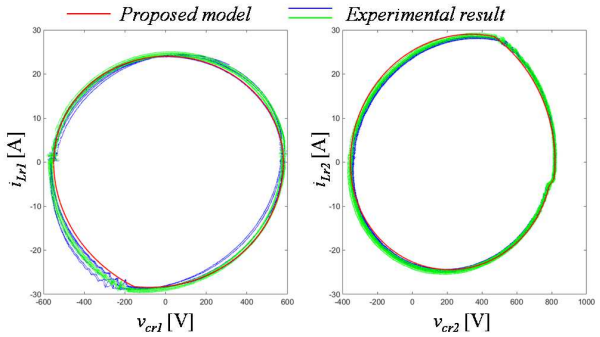

Fig. 8. Comparison of [v_{cr1}, i_{cr2}, v_2, i_2] between the proposed time domain model and the experimental results on V-I state plane

Figure 7 shows the comparison of [v_1, i_1, v_2, i_2] between the experimental results and simulation. It was verified that the operation of the converter through simulation and the actual experimental results were well identical. Figure 8 represents the comparison of [v_1, i_1, v_2, i_2] between the between the proposed time domain model and the experimental results on V-I state plane. In V-I state plane, an inflection point according to the mode change can be founded, and it can be confirmed that the voltage and current of the resonance element mostly coincide. In conclusion, considering the asymmetry of the actual manufactured resonant network and slight operating point errors, the proposed time domain model can be utilized. These results demonstrate that the proposed time domain model accurately predicts the operation of the actual system. The proposed model can provides a more reliable modeling method for the design and analysis of resonant CLLLC converters.

V. Conclusion

In this study, the proposed time domain model for the PWM mode of the CLLLC converter was analyzed and validated through simulation and experimental results. The comparison between the proposed time domain model and the experimental results demonstrated a high degree of accuracy, confirming the validity of the proposed model. In the V-I state plane analysis, the proposed model predicted the inflection points corresponding to mode changes, aligning closely with experimental observations. These findings indicate that the proposed time domain model is a reliable tool for designing and analyzing resonant CLLLC converters on PWM mode. Consequently, the proposed model can enhance the efficiency and accuracy of PWM mode resonant converter design processes in practical applications.

Acknowledgment

This research was supported by the Korea Research Institute for defense Technology(KRIT) grant, which is funded by the Korean government(DAPA) (C230027, Project for component localization)

This work was partly supported by Korea Institute of Energy Technology Evaluation and Planning(KETEP) grant funded by the Korea government (MOTIE) (No.20210501010020, Development on MMC-based ESS and Core Devices of High Voltage Hub-Station Grid Connected with Renewable Energy Source)

References

[1] H. Tu, H. Feng, S. Srdic, and S. Lukic, "Extreme Fast Charging of Electric Vehicles: A Technology Overview," IEEE Transactions on Transportation Electrification, vol. 5, no. 4, pp. 861–878, Dec. 2019

[2] Z. U. Zahid, Z. M. Dalala, R. Chen, B. Chen, and J. S. Lai, "Design of bidirectional DC-DC resonant converter for Vehicle-to-Grid (V2G) applications," IEEE Transactions on Transportation Electrification, vol. 1, no. 3, pp. 232–244, Oct. 2015

[3] J. H. Jung, H. S. Kim, M. H. Ryu, and J. W. Baek, "Design methodology of bidirectional CLLC resonant converter for high-frequency isolation of DC distribution systems," IEEE Trans Power Electron, vol. 28, no. 4, pp. 1741–1755, Apr. 2013, doi: 10.1109/TPEL.2012.2213346.

[4] W. Hua, H. Wu, Z. Yu, Y. Xing and K. Sun, "A Phase-Shift Modulation Strategy for a Bidirectional CLLC Resonant Converter," 2019 10th International Conference on Power Electronics and ECCE Asia (ICPE 2019 - ECCE Asia), Busan, Korea (South), 2019, pp. 1-6

[5] T. Zhu, F. Zhuo, F. Zhao, F. Wang, H. Yi, and T. Zhao, "Optimization of Extended Phase-Shift Control for Full-Bridge CLLC Resonant Converter with Improved Light-Load Efficiency," IEEE Trans Power Electron, vol. 35, no. 10, pp. 11129–11142, Oct. 2020, doi: 10.1109/TPEL.2020.2978419.

[6] X. Tang, Y. Xing, H. Wu, and J. Zhao, "An improved LLC resonant converter with reconfigurable hybrid voltage multiplier and PWM-Plus-PFM hybrid control for wide output range applications," IEEE Trans Power Electron, vol. 35, no. 1, pp. 185–197, Jan. 2020, doi: 10.1109/TPEL.2019.2914945.

[7] M. Young, The Technical Writer's Handbook. Mill Valley, CA: University Science, 1989.

[8] J. W. Kim and P. Barbosa, "PWM-Controlled Series Resonant Converter for Universal Electric Vehicle Charger," IEEE Trans Power Electron, vol. 36, no. 12, pp. 13578–13588, Dec. 2021, doi: 10.1109/TPEL.2021.3072991.

APPENDIX

Continuous conditions between *Mode* (a) and *Mode* (b)

$$\begin{cases} v_{crd}(\frac{T_s}{2}) = (V_{crd}(0) - v_{ka}) \cdot \cos \omega_r \frac{T_s}{2} \\ \qquad + \omega_r L_r i_d(0) \cdot \sin \omega_r \frac{T_s}{2} + v_{ka} \\ i_d(\frac{T_s}{2}) = -C_r \omega_r (V_{crd}(0) - v_{ka}) \cdot \sin \omega_r \frac{T_s}{2} \\ \qquad + i_d(0) \cdot \cos \omega_r \frac{T_s}{2} \end{cases} \tag{A1}$$

$$\begin{cases} v_{crs}(\frac{T_s}{2}) = (V_{crs}(0) - v_{ha}) \cdot \cos \omega_m \frac{T_s}{2} \\ \qquad + \omega_m L_{rm} i_s(0) \cdot \sin \omega_m \frac{T_s}{2} + v_{ha} \\ i_s(\frac{T_s}{2}) = -C_r \omega_m (V_{crs}(0) - v_{ha}) \cdot \sin \omega_m \frac{T_s}{2} \\ \qquad + i_s(0) \cdot \cos \omega_m \frac{T_s}{2} \end{cases} \tag{A2}$$

Continuous conditions between *Mode* (b) and *Mode* (c)

$$\begin{cases} v_{crd}(d_B T_s) = (V_{crd}(\frac{T_s}{2}) - v_{kb}) \cdot \cos \omega_r \left(d_B T_s - \frac{T_s}{2} \right) \\ \qquad + \omega_r L_r i_d(\frac{T_s}{2}) \cdot \sin \omega_r \left(d_B T_s - \frac{T_s}{2} \right) + v_{kb} \\ i_d(d_B T_s) = -C_r \omega_r (V_{crd}(\frac{T_s}{2}) - v_{kb}) \cdot \sin \omega_r \left(d_B T_s - \frac{T_s}{2} \right) \\ \qquad + i_d(\frac{T_s}{2}) \cdot \cos \omega_r \left(d_B T_s - \frac{T_s}{2} \right) \end{cases} \tag{A3}$$

$$\begin{cases} v_{crs}(d_B T_s) = (V_{crs}(\frac{T_s}{2}) - v_{hb}) \cdot \cos \omega_m \left(d_B T_s - \frac{T_s}{2} \right) \\ \qquad + \omega_m L_{rm} i_s(\frac{T_s}{2}) \cdot \sin \omega_m \left(d_B T_s - \frac{T_s}{2} \right) + v_{hb} \\ i_s(d_B T_s) = -C_r \omega_m (V_{crs}(\frac{T_s}{2}) - v_{hb}) \cdot \sin \omega_m \left(d_B T_s - \frac{T_s}{2} \right) \\ \qquad + i_s(\frac{T_s}{2}) \cdot \cos \omega_m \left(d_B T_s - \frac{T_s}{2} \right) \end{cases} \tag{A4}$$

Continuous conditions between *Mode* (c) and *Mode* (d)

$$\begin{cases} v_{crd}(T_0) = (V_{crd}(d_B T_s) - v_{kc}) \cdot \cos \omega_r (T_0 - d_B T_s) \\ \qquad + \omega_r L_r i_d(d_B T_s) \cdot \sin \omega_r (T_0 - d_B T_s) + v_{kc} \\ i_d(T_0) = -C_r \omega_r (V_{crd}(d_B T_s) - v_{kc}) \cdot \sin \omega_r (T_0 - d_B T_s) \\ \qquad + i_d(d_B T_s) \cdot \cos \omega_r (T_0 - d_B T_s) \end{cases} \tag{A5}$$

$$\begin{cases} v_{crs}(T_0) = (V_{crs}(d_B T_s) - v_{hc}) \cdot \cos \omega_m (T_0 - d_B T_s) \\ \qquad + \omega_m L_{rm} i_s(d_B T_s) \cdot \sin \omega_m (T_0 - d_B T_s) + v_{hc} \\ i_s(T_0) = -C_r \omega_m (V_{crs}(d_B T_s) - v_{hc}) \cdot \sin \omega_m (T_0 - d_B T_s) \\ \qquad + i_s(d_B T_s) \cdot \cos \omega_m (T_0 - d_B T_s) \end{cases} \tag{A6}$$

Continuous conditions between *Mode* (d) and *Mode* (a)

$$\begin{cases} v_{crd}(0) = (V_{crd}(T_0) - v_{kd}) \cdot \cos \omega_r (T_s - T_0) \\ \qquad + \omega_r L_r \cdot i_d(T_0) \cdot \sin \omega_r (T_s - T_0) + v_{kd} \\ i_d(0) = -C_r \omega_r (V_{crd}(T_0) - v_{kd}) \cdot \sin \omega_r (T_s - T_0) \\ \qquad + i_d(T_0) \cdot \cos \omega_r (T_s - T_0) \end{cases} \tag{A7}$$

$$\begin{cases} v_{crs}(0) = (V_{crs}(T_0) - v_{hd}) \cdot \cos \omega_m (T_s - T_0) \\ \qquad + \omega_m L_{rm} i_s(T_0) \cdot \sin \omega_m (T_s - T_0) + v_{hd} \\ i_s(0) = -C_r \omega_m (V_{crs}(T_0) - v_{hd}) \cdot \sin \omega_m (T_s - T_0) \\ \qquad + i_s(T_0) \cdot \cos \omega_m (T_s - T_0) \end{cases} \tag{A8}$$